Twisted chains of resonant particles: optical polarization control, waveguidance, and radiation

D. Van Orden,[1,*] Y. Fainman,[1] and V. Lomakin[1,2]

[1]*Department of Electrical and Computer Engineering, University of California, San Diego, La Jolla, California 92093-0407, USA*

[2]*e-mail: vitaliy@ece.ucsd.edu*

**Corresponding author: dvanorden@physics.ucsd.edu*

Received April 5, 2010; revised June 15, 2010; accepted June 25, 2010;
posted July 8, 2010 (Doc. ID 126367); published July 26, 2010

Linear chains of metallic nanoparticles that are sequentially rotated about the chain axis display interesting polarization-sensitive optical properties. Such twisted chains posses and extend properties of chiral gratings and general periodic gratings. They are characterized by high anisotropy and polarization sensitivity, and have subwavelength transverse dimensions. These structures are shown to support transverse modes with distinct propagation wavenumbers and radiation properties, including slow (bound) and fast (radiative) modes. They also have stop bands of different types, resulting from coupling between distinct transverse modes, as well as coupling with different higher-order diffraction modes. © 2010 Optical Society of America

OCIS codes: 130.5440, 250.5403, 050.6624, 130.2790.

Optical polarization control is important to the development of many integrated optical systems. Miniaturization of modern and future light-wave circuits demands the development of subwavelength devices, such as radiators, filters, and couplers, that are sensitive to the polarization of light. Existing optically active polarization devices include bulk media, such as liquid-crystal media [1], surface structures [2], and helical waveguides and fiber gratings [3,4]. Among those structures that support propagation and waveguidance, liquid crystals have relatively weak anisotropy, while helical fibers and waveguides cannot easily confine light to small dimensions, thus complicating dense integration. Realizing subwavelength optically active waveguiding and radiating structures is important to advance the development of dense nanophotonic systems.

In this Letter, we introduce and simulate "twisted" particle chain structures with strong polarization-sensitive propagation and radiation properties. The structures are composed of linear arrays of subwavelength metallic particles that are rotated sequentially about the array axis (Fig. 1). Such structures have several unique properties. Like all periodic nanoparticle chains [5–8], twisted chains support traveling waves that are mediated by strong interparticle interaction facilitated by plasmonic resonances. Introducing a sequential rotation to each nanoparticle, however, couples the otherwise independent transverse wave modes, resulting in modes with distinct polarization behavior. As a result, these structures (i) share certain polarization properties with chiral gratings [3], (ii) possess diffraction properties of general periodic gratings, (iii) have transverse dimensions of subwavelength size, and (iv) achieve high anisotropy and polarization sensitivity due to the particle resonances. These properties can have important applications to nanoscale optical devices. The presented analysis is also important to understand properties of general waveguiding and radiating structures.

We consider an infinite periodic chain of nonspherical resonant nanoparticles that are sequentially rotated about the chain axis by a constant angle ϕ_0 (Fig. 1). The chain lies on the z axis and has spacing d. The particles have polarizability tensor α, whose transverse principal values α_{xx} and α_{yy} are not equal. Twisted arrays similar to those in Fig. 1 can be fabricated, for example, using a force mediating polymer to bend silicon nanowires, which can be coated with metal [9]. In the arrangement of Fig. 1, the longitudinal traveling wave modes are independent and are not affected by the sequential rotation. We therefore restrict analysis to the transverse traveling wave modes and consider only the transverse field components.

A complete analysis of the radiation and propagation properties of modal fields supported by the structure in Fig. 1 can be performed using the discrete dipole approach with the dyadic periodic Green's function of the twisted array. In this approach, the chain elements are assumed to be small compared to the free-space wavelength λ. To find the source-free modal fields, all external source fields are set to zero. The dipole moment of the particle in the zeroth unit cell of the chain is therefore given by $\mathbf{p}_0 = \alpha \cdot \mathbf{E}_0$, where $\mathbf{E}_0$ is the electric field generated by all the rest of the particles in the chain. The dipole moment of all the chain elements have the same magnitude and are related to $\mathbf{p}_0$ via rotational matrices, determined by the chain twist angle, and via a phase shift between the elements that is determined by the modal wavenumber β. The electric field $\mathbf{E}_0$ is found as a superposition of contributions from the dipole moments as $\mathbf{E}_0 = \mathbf{G}_{\mathrm{rot}} \cdot \mathbf{p}_0$, where $\mathbf{G}_{\mathrm{rot}}$ is a rotated dyadic periodic Green's function accounting for the array's elements with rotation. This approach leads to the following self-consistency relation:

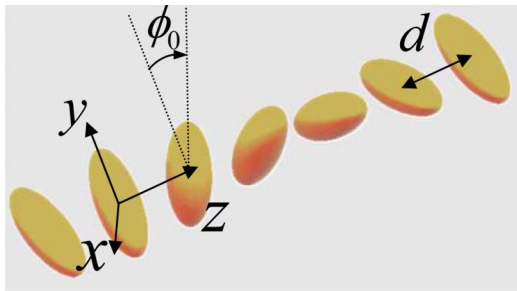

Fig. 1. (Color online) Twisted chain of nanoparticles with spacing d and twist angle ϕ_0.

 © 2010 Optical Society of America

$$(\mathbf{I}-\alpha\cdot\mathbf{G}_{\mathrm{rot}})\mathbf{p}_0=0,\qquad \mathbf{G}_{\mathrm{rot}}=\frac{1}{2}\begin{pmatrix} G_{xx}^{+}+G_{xx}^{-}-i(G_{xy}^{+}-G_{xy}^{-}) & G_{xy}^{+}+G_{xy}^{-}+i(G_{xx}^{+}-G_{xx}^{-}) \\ G_{yx}^{+}+G_{yx}^{-}-i(G_{yy}^{+}-G_{yy}^{-}) & G_{yy}^{+}+G_{yy}^{-}+i(G_{yx}^{+}-G_{yx}^{-}) \end{pmatrix}. \tag{1}$$

Here, the rotated dyadic Green's function is found via the elements of the matrices $\mathbf{G}^{\pm}=\mathbf{G}(k_0,\beta\pm\phi_0/d)$, where $\mathbf{G}(k_0,k_{z0})$ is the dyadic periodic Green's function of an infinite array of parallel dipoles with spacing d sequentially phase shifted by $k_{z0}d$. The observation point is taken to be the origin, and the source contribution of the particle located there removed so as to avoid self-interaction. It is given by $\mathbf{G}(k_0,k_{z0})=(1/4\pi\varepsilon)\sum_{n=-\infty,n\neq 0}^{\infty}e^{ik_{z0}nd}(k_0^2\overline{\overline{\mathbf{I}}}+\nabla\nabla)(e^{ik_0|\mathbf{r}-nd\hat{\mathbf{z}}|}/|\mathbf{r}-nd\hat{\mathbf{z}}|)|_{\mathbf{r}=\mathbf{0}}$, where $k_0=2\pi/\lambda$ is the free-space wavenumber. This lattice sum is slowly convergent but can be rapidly computed using certain spectral techniques, e.g., as in [10]. Self-consistency Eq. (1) can be solved for the (generally complex valued) modal wavenumber β and the corresponding ratio p_{x0}/p_{y0}.

The resulting modal fields have the same translation and rotation symmetry as the particle polarization states, though the symmetries are continuous, not discrete. The modal electric field may be expressed in two alternative forms:

$$\begin{aligned}\mathbf{E}(z\hat{\mathbf{z}})&=\left(\begin{pmatrix}\cos(\phi_0 z/d)\\ \sin(\phi_0 z/d)\end{pmatrix}E_{x0}\right.\\&\quad\left.+\begin{pmatrix}-\sin(\phi_0 z/d)\\ \cos(\phi_0 z/d)\end{pmatrix}E_{y0}\right)e^{i\beta z}\\&=E_R\begin{pmatrix}1\\ -i\end{pmatrix}e^{i\beta_R z}+E_L\begin{pmatrix}1\\ i\end{pmatrix}e^{i\beta_L z},\end{aligned}\tag{2}$$

where $\beta_R=\beta+\phi_0/d$ and $\beta_L=\beta-\phi_0/d$. The two expressions in Eq. (2) highlight different properties of the traveling wave modes. The first expression describes the mode propagation in terms of two rotating components and gives the field in the rotated coordinate system. The second expression, on the other hand, gives the modal field in terms of a left-handed circularly polarized (LCP) and a right-handed circularly polarized (RCP) component in the Cartesian coordinate system, and represents the fields as observed in a laboratory reference frame. The corresponding RCP and LCP wavenumbers are given by β_R and β_L, respectively. This latter expression reveals the radiation properties of the chain.

Self-consistency Eq. (1) may be solved numerically to find four source-free solutions in the first Brillouin zone (with respect to the periodicity d), representing two independent modes propagating in each direction. The modes with positive group velocity have wavenumbers $\beta=\beta^{+}$ and β^{-}, found near $k_0+\phi_0/d$ and $k_0-\phi_0/d$, respectively, while those with wavenumbers $-\beta^{+}$ and $-\beta^{-}$ have negative group velocity. Because of the structure periodicity d, the modal fields can be represented as a sum of an infinite number of diffraction (Floquet) modes whose wavenumbers $\beta_m^{\pm}=\beta^{\pm}+2\pi m/d$ (with m an integer) also solve Eq. (1) and correspond to source-free modal fields.

The modal fields can exhibit several types of behavior, resulting from the presence of the twist and the discrete periodicity, including stop bands of two types, propagation without radiation loss, and radiation of two types. Stop bands form for certain chain geometries and frequency ranges when two distinct modes with counterpropagating energy couple strongly. One way this can occur is through coupling of one of the four traveling wave modes mentioned above to a higher diffraction order of another one. For example, a stop band may form through coupling of first-order diffraction modes when $-\mathrm{Re}\{\beta^{\pm}\}+2\pi/d=\mathrm{Re}\{\beta^{\pm}\}$ or $-\mathrm{Re}\{\beta^{\pm}\}+2\pi/d=\mathrm{Re}\{\beta^{\mp}\}$. The strong mode coupling results from the interplay between the effects of the twisting with angle ϕ_0 and the periodicity d. Such interplay is absent in ordinary chiral gratings or periodic (nonchiral) gratings. Another way a stop band may form is through direct coupling between the $-\beta^{-}$ and β^{-} modes that occurs for sufficiently large ϕ_0/d when $\mathrm{Re}\{\beta^{-}\}=0$.

Figure 2(a) shows the dispersion curves for a chain of gold prolate spheroids embedded in a silicon dioxide medium with spacing $d=72$ nm and twist angle $\phi_0=18°$. The curves are found by tracking the real parts of β^{+} and β^{-} over a range of values of the free-space wavenumber k_0 for which waveguidance is supported. Two sets of curves are shown: one for realistic lossy gold particles whose permittivity is given by the Drude model with parameters chosen to match those given by Palik [11], and the other for lossless Drude gold particles with a vanishing damping constant. In both cases, the β^{+} mode couples to the first-order diffraction mode of $-\beta^{+}$, found at $-\beta^{+}+2\pi/d$. In the lossless case, for which β^{+} is a purely real number, it forms a clear stop band, located at $\beta^{+}d=\pi$, where the two solutions merge. In the lossy case, the two solutions have imaginary parts with opposite signs and remain separated; no sharp band edge forms, although the coupling is evident from the way the dispersion curve for β^{+} bends back away from the lossless stop-band point, indicating a change in group velocity. Figure 2(b) shows the dispersion diagram for lossy

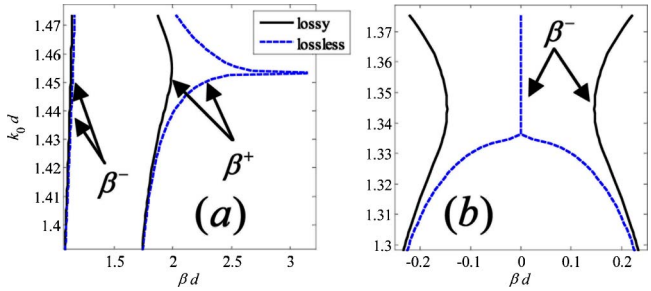

Fig. 2. (Color online) (a) Dispersion relations of the β^{+} and β^{-} modes for chains of lossless and lossy gold ellipsoids with spacing $d=72$ nm, twist angle $\phi_0=18°$, and major and minor axes of lengths of 34 and 17 nm, respectively. (b) Dispersion relations of the β^{-} mode for the same chain but with twist angle $\phi_0=85°$.

and lossless chains identical to those considered in Fig. 2(a) except for a larger twist angle, which is now $\phi_0 = 85°$. For the lossless chain, a stop band forms right at the origin, while for the lossy chain the curves bend away from each other.

The propagation and radiation properties of twisted chains are best described by the second expression in Eq. (2). First consider the case of sufficiently small d for which higher-order diffraction modes are not in the propagation range. Because $\beta^+ \pm \phi_0/d > k_0$, the β^+ mode is a slow wave that does not radiate and whose fields decay exponentially transverse to the chain. This mode is best excited by a source with an evanescent spectrum. The β^- mode, in contrast, is composed of an RCP wave with wavenumber $\beta_R^- = \beta^- + \phi_0/d > k_0$ and an LCP wave with wavenumber $\beta_L^- = \beta^- - \phi_0/d$, which can be either in the evanescent or propagating range. For small to moderate twist rates, $|\beta_L^-| < k_0$, and the mode is a leaky (fast) wave whose LCP component radiates out of chain at an angle θ_{rad} with the chain (z) axis. The radiation angle is approximately determined by the phase-matching condition $k_0 \cos(\theta_{\mathrm{rad}}) = \mathrm{Re}\{\beta^-\} - \phi_0/d$. It can be shown that the radiated beam has left-handed elliptical polarization with ellipticity (i.e., major-to-minor axis ratio) given by $e = \sec(\theta_{\mathrm{rad}})$. It follows from reciprocity that this mode may be excited by an LCP far-field source or by a source having an RCP evanescent spectrum (e.g., via a prism). If the particle spacing d is large enough for diffraction modes to enter the radiation range, the β^+ mode may also be leaky. As a result, the chain will radiate into multiple beams at distinct angles.

The predicted radiation characteristics of traveling wave modes may be verified by simulating a finite twisted chain. A finite structure cannot be analyzed using the periodic Green's function, but the Green's function for a single dipole source may be used to find the interaction among all the chain elements and solve for the induced dipole moment of each nanoparticle in response to an external source. Consider a chain of 200 particles with the same parameters as in the infinite case in Fig. 2. The chain is excited by an RCP-localized source placed on the z axis a distance $d = 72$ nm from the chain. Figure 3(a) shows the radiation pattern as a function of the observation angle θ with respect to the z axis far from the chain, where the far-field dominates. For this dense array, the radiation results solely from the chain twist. The pattern shows a clear peak at the angle θ_{rad} at which radiation from the β^- traveling wave mode is predicted for an infinite structure. The chain acts as a nanoscale leaky-wave antenna whose radiation angle and polarization may be tuned by varying the twist rate ϕ_0/d. Figure 3(b) shows the radiation pattern for a chain with twist angle $\phi_0 = 48°$ and a larger periodicity $d = 181$ nm. For this large spacing Floquet modes lead to radiation for the otherwise slow β^+ mode. Here, two peaks are observed with radiation angles θ_1 and θ_2 agreeing with the conditions $k_0 \cos(\theta_1) = \mathrm{Re}\{\beta^+\} - \phi_0/d - 2\pi/d$ and $k_0 \cos(\theta_2) = \mathrm{Re}\{\beta^+\} + \phi_0/d - 2\pi/d$.

In conclusion, we have analyzed the traveling wave modes of a linear chain of sequentially rotated nanoparticles. We have shown that two modes are found propagating in each direction and that, for sufficiently small spacings, one of these modes is a slow wave bound to the chain while the other is a fast wave that radiates. Furthermore, the structure's dispersion relations exhibit stop bands of two kinds: those associated with coupled diffraction modes and those resulting from oppositely propagating zero-order modes. These structures may have applications as subwavelength polarization-sensitive optical filters and antennas.

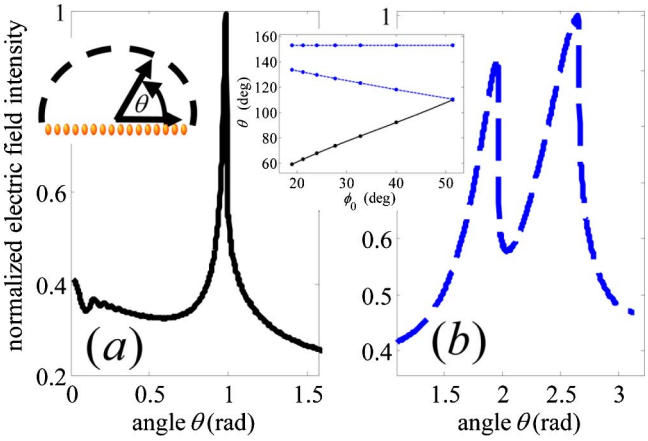

Fig. 3. (Color online) (a) Far-field radiation intensity observed a distance of 960 μm from a chain of 200 gold ellipsoids with spacing $d = 72$ nm, twist angle $\phi_0 = 18°$, excited by a localized RCP source with wavelength $\lambda = 527$ nm. (b) Radiation pattern from the same chain but with spacing $d = 181$ nm, twist angle $\phi_0 = 48°$, excited by an LCP localized source. Inset, radiation angle θ as a function of twist angle ϕ_0 for the radiated beam in (a) (bottom curve) and the two beams in (b) (top curves). The observed angles agree with the values predicted from the phase-matching equations with a relative error around 1%.

This work is supported by the Defense Advanced Research Projects Agency (DARPA) NACHOS program, and the National Science Foundation (NSF) CIAN center.

References

1. C. Oldano, E. Miraldi, and P. Taverna Valabrega, Phys. Rev. A **27**, 3291 (1983).
2. A. Papakostas, A. Potts, D. M. Bagnall, S. L. Prosvirnin, H. J. Coles, and N. I. Zheludev, Phys. Rev. Lett. **90**, 107404 (2003).
3. V. I. Kopp, V. M. Churikov, J. Singer, N. Chao, D. Neugroschl, and A. Z. Genack, Science **305**, 74 (2004).
4. G. Shvets, Appl. Phys. Lett. **89**, 141127 (2006).
5. M. L. Brongersma, J. W. Hartman, and H. A. Atwater, Phys. Rev. B **62**, R16356 (2000).
6. W. H. Weber and G. W. Ford, Phys. Rev. B **70**, 125429 (2004).
7. A. Alù and N. Engheta, Phys. Rev. B **74**, 205436 (2006).
8. D. Van Orden, Y. Fainman, and V. Lomakin, Opt. Lett. **34**, 422 (2009).
9. S. Walavalkar, A. Homyk, D. M. Henry, and A. Scherer, J. Appl. Phys. **107**, 124314 (2010).
10. D. Van and V. Lomakin, IEEE Trans. Antennas Propag. **57**, 1973 (2009).
11. E. D. Palik, *Handbook of Optical Constants of Solids* (Academic, 1998).